

ISTITUTO NAZIONALE FISICA NUCLEARE

INFN/AE - 81/1

30 gennaio 1981

G. Alberi:

NUCLEON NUCLEON DIFFRACTION

SERVIZIO RIPRODUZIONE DELLA  
SEZIONE DI TRIESTE DELL'INFN

NUCLEON NUCLEON DIFFRACTION

G. Alberi

Istituto di Fisica Teorica, Università di Trieste, Italy  
Istituto Nazionale di Fisica Nucleare, Sezione di Trieste, Italy

Seminar given in the I.N.F.N. High Energy Physics Groups of Milano and Pavia  
and Invited talk given in the National Meeting of Intermediate Energy Physics,  
Olinda (Recife), Brazil, 7-9 May 1980.

## ABSTRACT

In this paper we discuss the physical importance of nucleon-nucleon diffraction and the main differences with well understood nucleon nucleus diffraction. In the theoretical description of nucleon-nucleon diffraction in terms of the eikonal model, the hypothesis of factorization is shown to be in contradiction with the energy dependence of the impact parameter profile in proton-proton scattering at CERN -ISR. This dependence is highly non-uniform in impact parameter, giving rise to a pronounced peripheral increase with energy of the inelastic overlap function.

Two experimental findings in inelastic diffraction indicate the existence of a deep relation of this process with the peripheral increase of the profile function. The first refers to the clear-cut proof that inelastic diffraction is peripheral in impact parameter space, in coherent production on deuteron. The second is the analysis of the integrated cross sections for inelastic diffraction, which leads to the conclusion that most of the total cross section increase in the ISR energy range comes from this process.

It is then clear that the eikonal model should be modified in order to include inelastic diffraction. A recent trial in this direction by Miettinen and Thomas shows the existence of a substantial difference between the matter and the charge distribution inside the proton. Their result favours a description of the proton in terms of the string model.

## 1. INTRODUCTION

Diffraction is a well known phenomenon in classical physics, and occurs whenever waves encounter obstacles or holes with dimensions large compared with their wave length. The signature is the presence of minima and maxima in the intensity of the wave, after having interacted with the obstacle or the hole.

This phenomenon appears also in nucleon-nucleon elastic scattering at very high energies, where the differential cross section presents a clear minimum and a secondary maximum, as shown on fig. 1a.

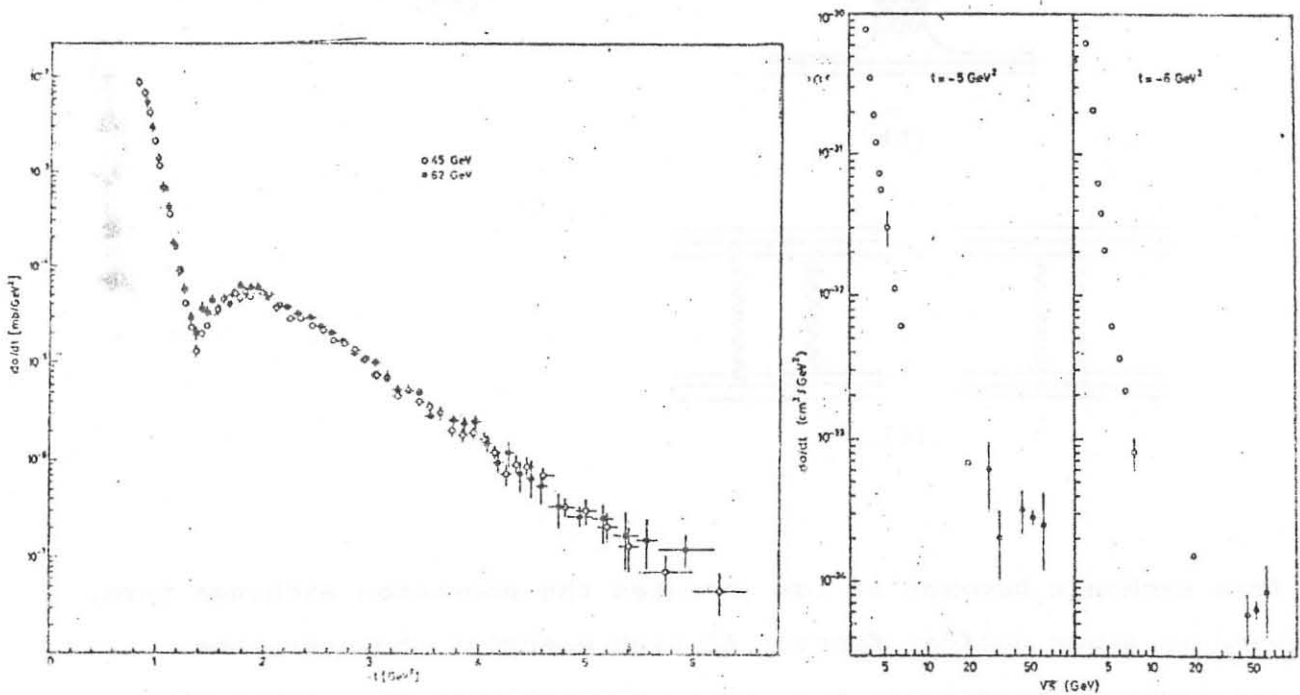


Fig. 1 a) Differential cross section for elastic proton-proton scattering two ISR energies  $\sqrt{s} = 45$  and  $63$  GeV. The data at higher energies are scaled down according to geometrical scaling.

b) behaviour with energy of  $d\sigma/dt$  for proton-proton elastic scattering at fixed values of  $|t| = 4$  and  $6$  GeV<sup>2</sup>.

This phenomenon becomes dominant only at laboratory energies of the order of 100 GeV/c because for lower energies, the dominant process is the exchange of Regge poles, which can be interpreted as the exchange of a quark-antiquark pair (Fig. 2a)

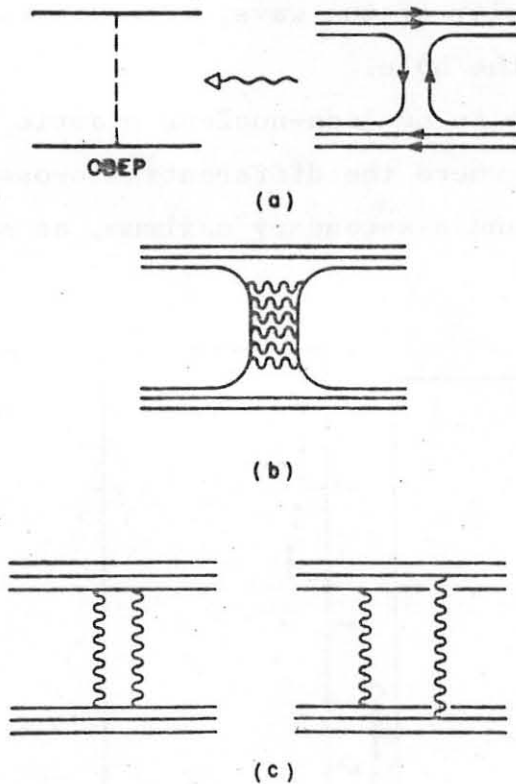


Fig. 2. Quark diagrams for Regge exchange (a) (b) and for diffraction (c).

This exchange becomes at low energies the one-boson exchange term, used to study nuclear forces. At high energies, however, the amplitude is reggeized, i.e. it is proportional to a power of  $s$ .

$$f_{\text{Regge}} \sim s^{\alpha(t)} \quad (1)$$

where  $\alpha(t)$  is the Regge trajectory. These trajectories are linear and have intercept  $\alpha(0)$  less than 1 (for instance  $\alpha_p(0) = \alpha_\omega(0) = 1/2$  and  $\alpha_\pi(0) = 0$ ). Therefore the corresponding contribution to the total cross section

$$\sigma_t \sim S^{\alpha(0) - 1} \quad (2)$$

is decreasing as an inverse power of  $S$ . The physical interpretation of this feature, although not yet completely clear, is that the Regge pole exchange corresponds to a quark-anti-quark pair in the  $t$ -channel with the same quantum numbers of the corresponding elementary particles, but with a structure of many gluon exchanges representing the production of many particles in the inelastic channel. In other words, as the energy increases, the acceleration of the quarks increases and the bremsstrahlung of gluons becomes more important contributing in this way more to the inelastic channels at the expenses of the elastic one<sup>1)</sup>. The decrease with the energy of this contribution can be seen plotting the proton-proton elastic differential cross section as a function of the Center of Mass energy for fixed values of the momentum transfer. This is shown in fig. 1.b, where the Regge pole contribution is rapidly decreasing until  $\sqrt{s} = 30$  GeV and the scaling diffraction term becomes clearly visible for higher energies.

From the analogy with classical physics, we expect that diffraction depends only on the form of the quark distributions inside the proton, being essentially independent from the incident energy.

This last process can be represented in terms of the exchange of at least two gluons (fig. 2c), which is the minimum number to form a color singlet. This mechanism has been studied<sup>2)</sup> in the framework of the MIT bag model and was shown to give a total cross section constant with energy. Furthermore the value of the coupling constant  $\alpha_s$  at the quark gluon vertex consistent with the experimental value of the proton-proton total cross section is small. This is in agreement with the main assumption of the MIT bag model, where the quarks are constrained to be inside the bag by an outside pressure, but are essentially free.

As a matter of fact, the energy dependence of proton-proton differential cross section is only approximately constant. The slow energy dependence, best represented in terms of  $\ln s$ , is discussed in the following. An even more detailed discussion can be found in ref. 3, where most of the following material is coming from.

If we forget for a moment the fine details of the energy dependence, elastic scattering in proton-proton presents very similar features to nucleon-nucleus or nucleus-nucleus scattering. In first approximation one can describe the elastic scattering amplitude in terms of the black sphere model

$$f_{el}(q) \sim iR^2 \frac{J_1(qR)}{qR} \quad (3)$$

where  $R \sim 1f$ . This model is consistent with the zero in the differential cross section at  $t = 1.4 \text{ GeV}^2$  corresponding to the first zero of the  $J_1$  Bessel function. This parametrization is clearly appropriate for nucleus-nucleus elastic scattering, but the value of the interaction radius has to be larger and depends on the mass number of the nucleus.

This similarity is to be contrasted with two striking differences in inelastic diffraction

a) while for nuclear inelastic diffraction the differential cross section for the inelastic process has an evident suppression at  $0^\circ$  diffusion angle there is no sign of this structure in the corresponding process for proton excitation. This is shown in fig. 3a and b.

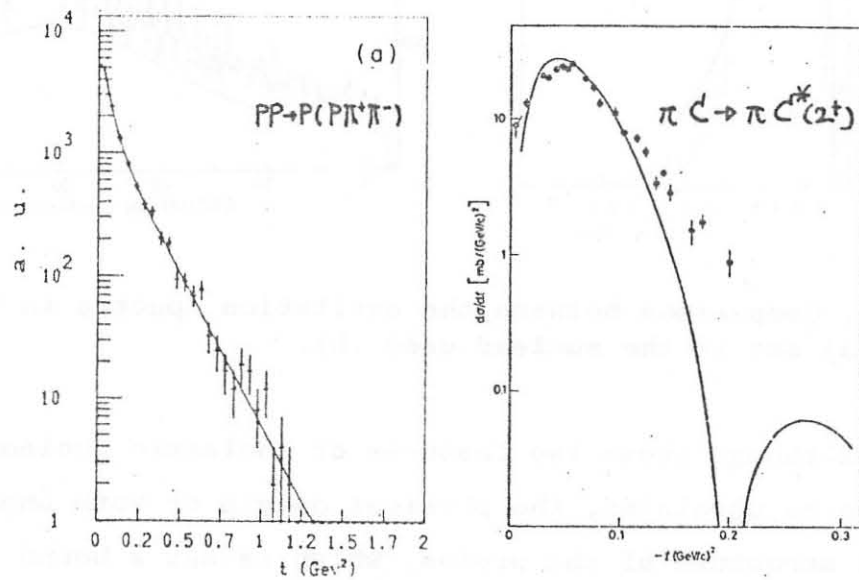


Fig. 3 Comparison between differential cross sections for inelastic diffraction in the nucleon case (a) and in the nuclear case (b).

b) while for nuclear inelastic diffraction, the excitation spectrum is mainly discrete with a small background, the mass spectrum in nucleon diffractive excitation is mainly continuum with few discrete peaks superimposed. This is shown in fig. 4a and b.



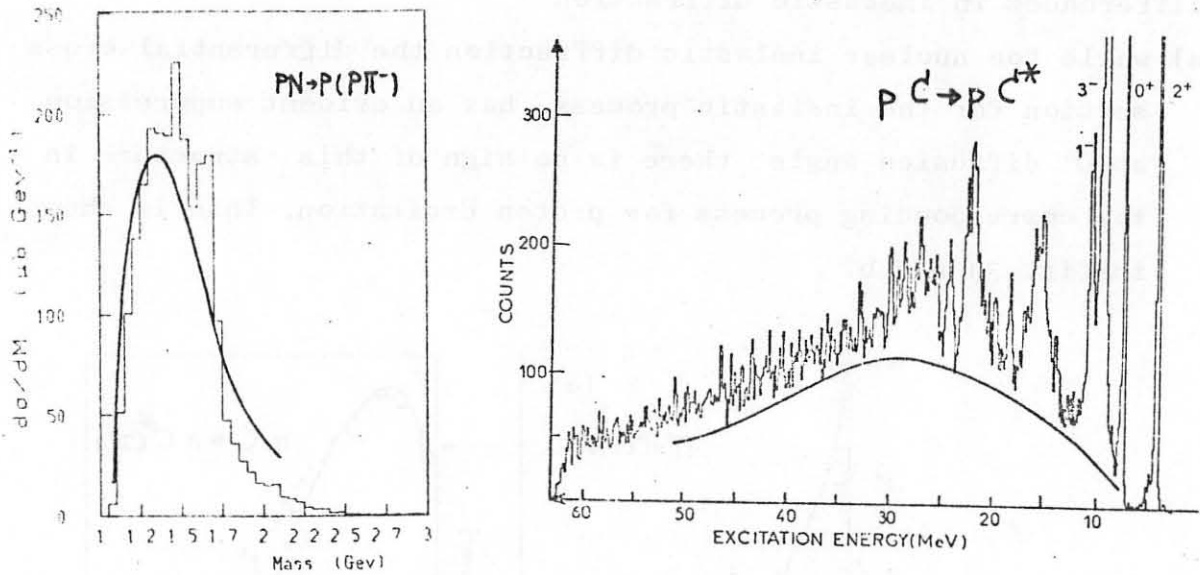


Fig. 4. Comparison between the excitation spectra in the nucleon case (a) and in the nuclear case (b).

Although these two features of inelastic nucleon diffraction seem to be unrelated, the physical origin of both phenomena is found in the structure of the proton, which is not a bound state of a many body system with well defined constituents as nuclei, but is a field configuration showing large fluctuations in its structural properties. One can say in other words that the proton is not only a bound state of three quarks, but it is also a source of gluons, fluctuating in their number and their space configuration. This picture can be made more precise in the framework of the Good and Walker<sup>4)</sup> formalism. This consist in assuming that the incident proton is a superposition of states, which are eigenstates of the  $T$  matrix

$$|P\rangle = \sum_{\alpha} c_{\alpha} |\psi_{\alpha}\rangle \quad (4)$$

$$T |\psi_{\alpha}\rangle = t_{\alpha} |\psi_{\alpha}\rangle$$

where the  $t$  matrix is assumed to be completely imaginary and therefore is an hermitian operator apart from the factor . This assumption implies that each state  $|\Psi_k\rangle$  is absorbed in a different way by the interaction, according to its corresponding eigenvalue, causing in this way the transition to a different superposition of states  $|\Psi_k\rangle$ , which is the excited state of the proton. A similar phenomenon occurs in the absorption of partially polarized light in a medium, where the imaginary part of the refraction index depends on the polarization<sup>5)</sup>. After going through the medium, the light is still partially polarized but in a different way.

This formalism can be implemented in the parton model, assuming that each state  $|\Psi_k\rangle$  is defined by the number of wee<sup>6)7)</sup> partons present in the proton structure and by their space configurations

$$|\Psi_k\rangle = |\vec{b}_1, \dots, \vec{b}_N, y_1, \dots, y_N\rangle \quad (5)$$

where  $N$  is the number of wee partons,  $\vec{b}_i$  are their transverse coordinates and  $y_i$  their rapidities. A formalism of this type<sup>7)</sup> is able to reproduce the diffractive peak, showing that it is just the fluctuation in the number of wee partons, which is the responsible of the existing difference between the nucleon and the nuclear case for the differential cross section at  $|t| = 0$ .

The same fluctuations are probably responsible for pion emission, which reproduces the continuum background shown as continuous line in fig.4. Pion emission is supposedly the result of gluon emission, quark antiquark pair production and finally a hadronization of a singlet quark-antiquark pair out of a fluctuating sea of quarks and gluon (see fig. 5).

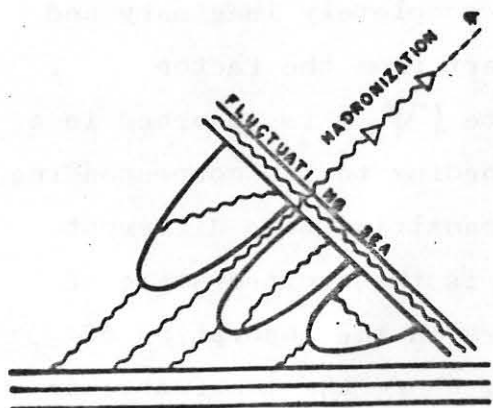


Fig. 5

Fig. 5.  
Schematic representation of  
the fluctuating sea partons,  
generating off shell pions.

The conclusion is then that it is the field theoretical structure of the proton which is responsible for the main differences between nuclear and nucleon inelastic diffraction. This structure should be taken in account also in elastic scattering, for which a simple nuclear description fails to describe the energy dependence of the impact parameter profile for proton-proton elastic scattering . This will be discussed in the following.

2. Eikonal model: theoretical and phenomenological problems

The eikonal model for nucleon-nucleon elastic scattering<sup>8)</sup> is based on the assumption that the eikonal function, in the Fourier-Bessel transform of the elastic amplitude, is the overlap of the matter densities of the colliding nucleons (See fig. 6).

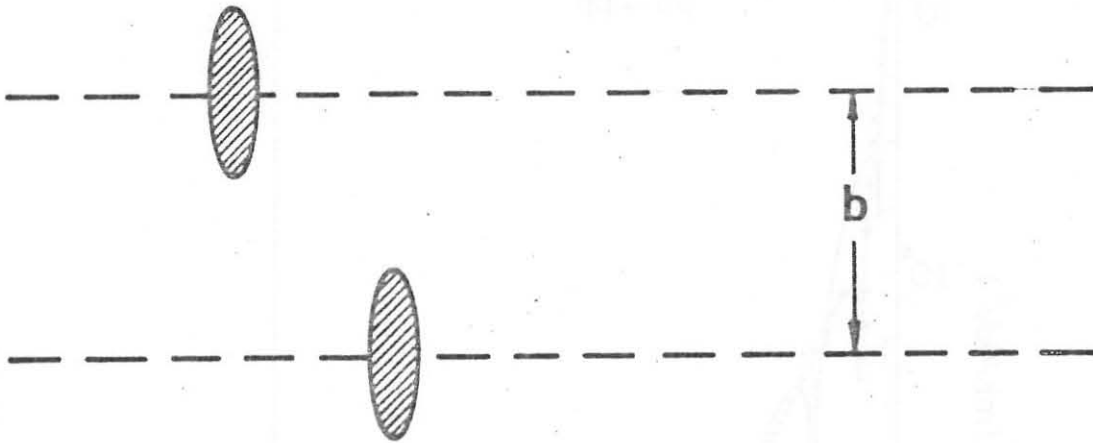


Fig. 6 Collision of two relativistically contracted protons at impact parameter  $b$ .

This gives

$$F(q) = \frac{i}{2\pi} \int d^2b e^{i\vec{q} \cdot \vec{b}} \left[ 1 - e^{-\mu_0 \int p(\vec{b}-\vec{b}') p(\vec{b}') d^2b'} \right] \quad (6)$$

where  $\rho(\vec{x})$  is the matter density of the proton, and  $\mu_0$  is a free parameter, which stands for the strength of the interaction. In the original formulation of this model<sup>8)</sup>, one further assumption was that the matter density is equivalent to the charge density of the proton. This could be justified on the experience in nuclear diffraction,

where the two distributions turn out to be very similar<sup>9)</sup>.

Actually the original formulation of the model was able to reproduce the main features of the low  $|t|$  differential cross section, that is the diffractive peak, the minimum at  $|t| = 1.4$   $\text{GeV}^2$  and the second maximum.

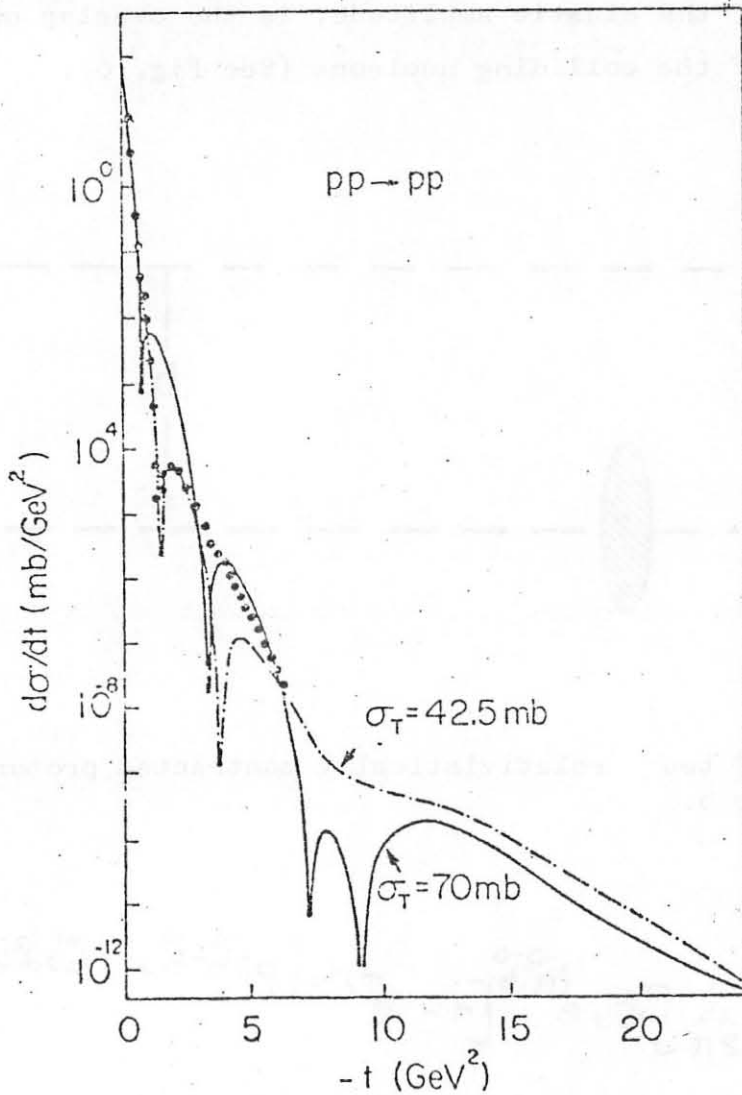


Fig. 7 Proton-proton elastic differential cross section and prediction of the eikonal model in its original formulation for two different values of the proton-proton total cross section<sup>3)</sup>.

The failure of this model at large values of  $|t|$  (fig. 7) stimulated the generalization of the model, where the matter densities have a spin structure and the different components are related to the charge and the magnetization densities. This can be generally formulated as <sup>10)</sup>

$$S(b) = \alpha P \left\{ - \sum_a \mu_a \int d^2 b' J_4^{a_k}(\vec{b}-\vec{b}') J_4^{a_k}(\vec{b}') \right\} \quad (7)$$

where  $k$  is a general index, which is the isospin index in ref. 10 and is referring to the convection current and the spin current in ref. 11. Since the current is expressed as

$$\langle \vec{p}' s' | J_\mu(x) | \vec{p} s \rangle = \alpha P [i(\vec{p}-\vec{p}') \times] \frac{e u}{\sqrt{p_0 p_0'}} \bar{u}(\vec{p}' s') \left[ F_1(t) \gamma_\mu + i \sigma_{\mu\nu} (\vec{p}' - \vec{p})^\nu \frac{F_2(t)}{2m} \right] u(\vec{p} s) \quad (8)$$

this theory predicts a non zero polarization for proton-proton scattering <sup>12)</sup>; this means that any theory of this type should be compared with existing polarization data <sup>13)</sup>.

Even if these theories are quite successfull in fitting the differential cross section for proton-proton elastic scattering, it remains to be understood why the eikonal function is given by the overlap of the two matter distribution. One possible way to justify it, is to assume that the matter density comes from the spatial distribution of the proton constituents, as it is done for nuclear scattering in Glauber theory, and take a zero range interaction between the constituents of the two protons. This procedure is common in nuclear physics, where the range of the nucleon-nucleon interaction is much smaller than the nuclear size; it is not clear why this should be true here, where we know that elementary interactions are weak at small distances and increase with the distance (asymptotic freedom), so that the range of the elementary

interaction should be of the same order of the proton size.

But even if one accepts this hypothesis, it is difficult to understand the equivalence between matter and charge distribution in the simplest case and the representation of the matter overlap in terms of the electromagnetic currents in the most general case. This is because gluons are continuously emitted and absorbed in a confined quark state and they certainly take part in the interaction through gluon exchange, thanks to the important triple gluon coupling.

These fluctuating gluons are neutral to electromagnetic interactions and they are not necessarily distributed in space according to the charge distribution, so that the overall matter distribution could be substantially different from the charge distribution.

These considerations leave serious doubts on the validity of the assumptions which lie under the eikonal model and its more advanced formulations.

The original model, as formulated in eq. 6, contains the energy dependence in a factorized way, that is while the overlap integral is energy independent the parameter  $M_0$  can be varied in order to reproduce the energy dependence of the total cross section. This factorization is not reproduced in the energy variation of the impact parameter representation of the proton-proton differential cross section<sup>14,15,16</sup>). The procedure consists in calculating the real part of the scattering amplitude using relations and subtract its contribution from the differential cross section so that we can write the imaginary part of the scattering amplitude as a Fourier-Bessel transform

$$i \text{Im} F(t) = i \sqrt{\frac{1}{\pi}} \left( \frac{d\sigma}{dt} - R^2(t) \right) = \frac{i}{2\pi} \int e^{i\vec{q}\cdot\vec{b}} (1 - e^{-\Omega(s,b)}) d^2b \quad (9)$$

where  $\Omega(s,b)$  is called the opacity function, which corresponds

to the imaginary part of the eikonal function in potential scattering and it is therefore responsible for the absorption in the scattering process.

For the eikonal model of eq. (6), the opacity function has a factorized dependence on  $s$  and  $b$

$$\Omega(s, b) = \mu_0(s) f(b) \quad (10)$$

that is the logarithmic derivative in  $\ln s$  does not depend on  $b$ .

$$\frac{d \ln \Omega(s, b)}{d \ln s} = \frac{d \ln \mu_0}{d \ln s} \quad (11)$$

The energy variation of the "experimental" opacity function<sup>16)</sup> is showing a clear linear dependence on  $b$  of the logarithmic derivative (see fig. 8).

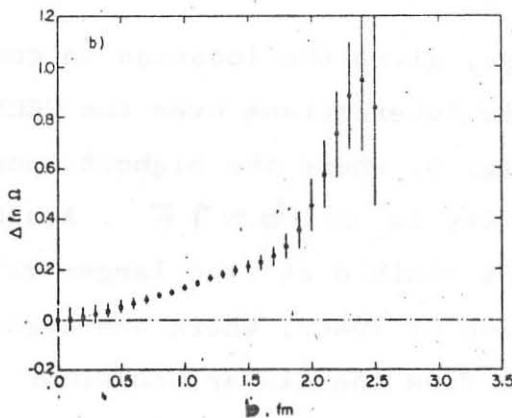


Fig. 8 Logarithmic derivative of the opacity function  $\Omega(s, b)$  with respect to  $\ln s$  as function of  $b$  16).

This linear dependence breaks down at large values of the impact parameter  $b$ , where the dependence becomes stronger and could be quadratic in  $b$ . These large values of  $b$  correspond to the smallest  $|t|$  values and the anomaly is probably associated with the breaking of the exponential behaviour of the differential



cross section<sup>3)</sup>.

The knowledge of the Fourier-Bessel transform of the elastic scattering amplitude

$$P(b) = 1 - e^{-\sqrt{2}(s,b)} \quad (12)$$

is sufficient for determining through the unitarity relation in space

$$2P(b) = |P(b)|^2 + G_{im}(b) \quad (13)$$

the probability density for inelastic interaction usually called overlap function.

The function<sup>16)</sup>

$$\Delta G_{im}(s,b) = G_{im}(s,b) - G_{im}(s_0,b) \quad (14)$$

where  $s_0$  is a reference energy, gives the location in coordinate space of the increase of inelastic interactions over the CEFN-ISR energy range. This is shown in fig. 9, where the highest increase in inelastic interaction probability is at  $b \sim 1F$ . Another peak in the function  $\Delta G_{im}$  is visible at even larger values of  $b \sim 2F$ , in the same region of space, where the logarithmic derivative is showing a deviation from the linear behaviour in  $b$

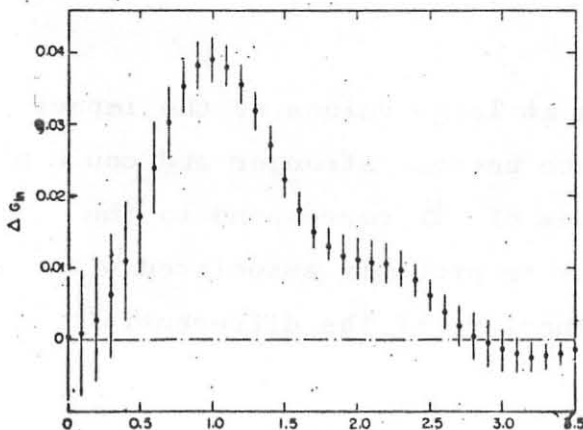


Fig. 9 The increase of the overlap function  $G_{im}(b)$  from the lowest to the highest ISR energy, as function of  $b$ .

This result establishes a relation between the linear behaviour of the logarithmic derivative of the opacity function and the peripheral increase of the inelastic overlap function, so that the origin of the deviation from the factorization in the eikonal function comes from an inelastic process. Two experimental facts about inelastic diffraction indicate in this process the physical reason for the linear dependence of the logarithmic derivative of the opacity function, as discussed in details in the following.

### 3. TWO EXPERIMENTAL FACTS ABOUT INELASTIC DIFFRACTION

Why a peripheral increase of the inelastic interaction probability? Two experimental observations establish a strong link between this fact and inelastic diffractive. These are

- a) a large increase with energy of the total cross-section for inelastic diffraction, accounting for most of the total cross section increase over the ISR energy range
- b) the peripheral character of inelastic diffraction, recently proved experimentally in coherent production on deuteron.

The first observation comes from the compilation of the integrated cross section data for single diffraction and double diffraction together with the factorization predictions for double diffraction shown on fig. 10. Even if the errors are quite large, there is a clear evidence for a substantial increase over the ISR energy range, which amount to about 4 mb in the sum of the two integrated cross sections; since the total cross section increase is about 5 mb, this shows that even taking in account the errors, inelastic diffraction plays an important role in the total cross section increase.

This last statement receives new support from the observation of the peripheral location in b-space of inelastic diffraction. This observation can be done using the deuteron as interferometer, as it was proposed some time ago<sup>17)</sup>. This method, which could be called "hadron interferometry" consist in observing the interference

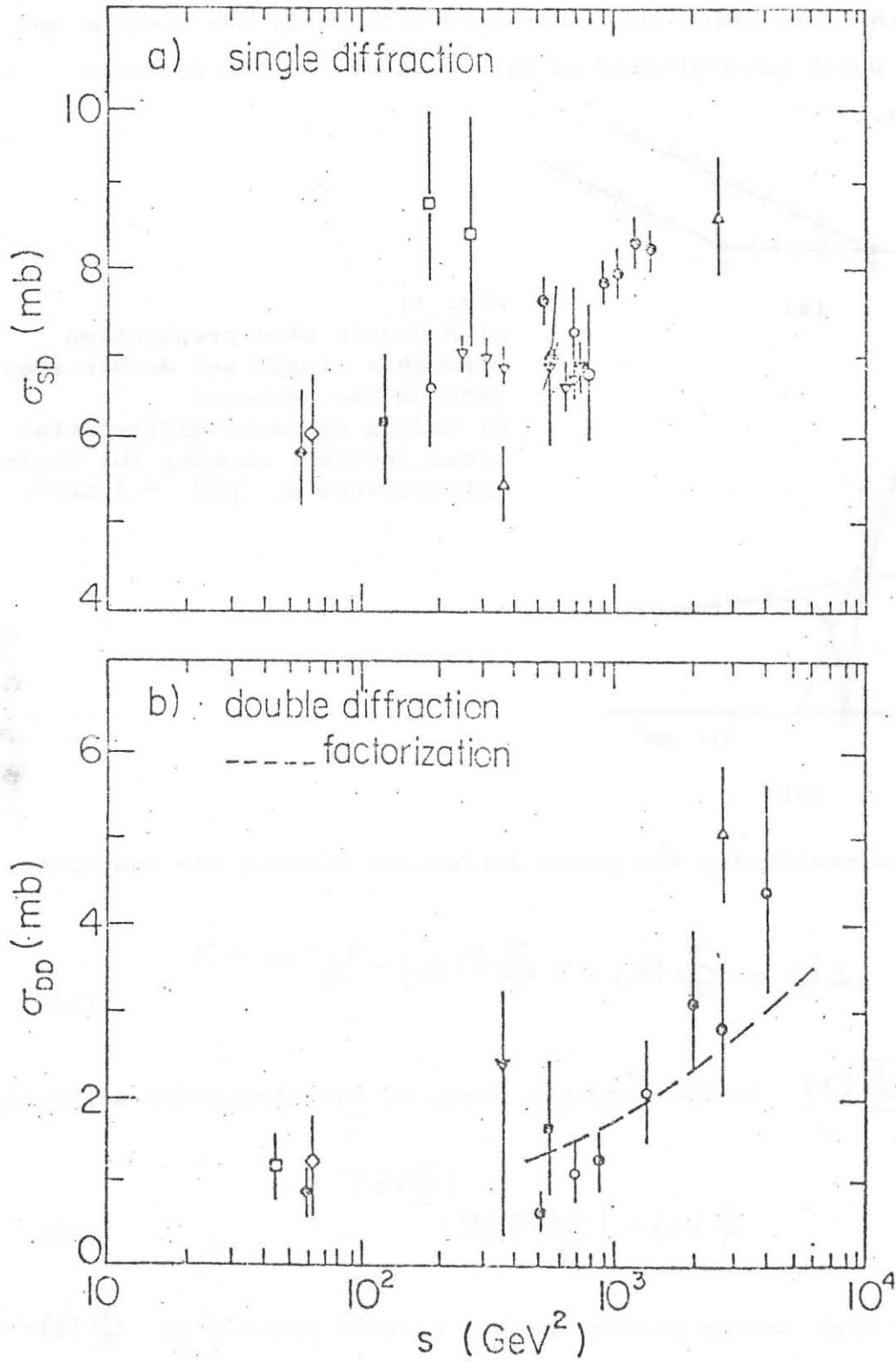
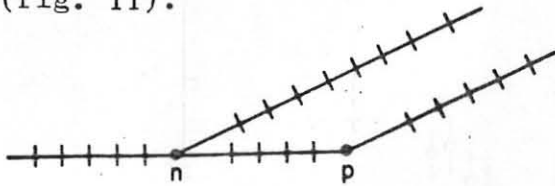


Fig. 10 Energy dependence of total inelastic diffraction in proton-proton interaction<sup>3)</sup>.

between the wave which has interacted with only one nucleon and the wave which has scattered on both nucleons of the deuteron (fig. 11).

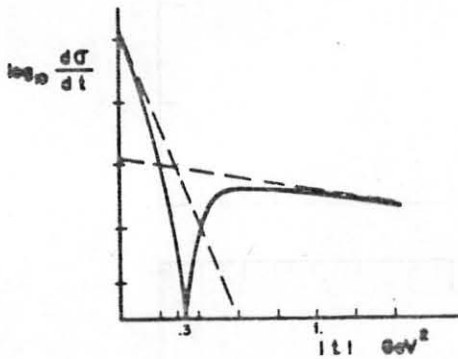


(a)

Fig. 11

a) Hadronic wave propagation through a single and double step path on the deuteron

b) Hadron deuteron differential cross section, showing the maximum interference at  $|t| = .3 \text{ GeV}^2$ .



(b)

In elastic scattering the phase difference between the two waves is

$$\Delta\varphi = \Phi(t) - 2\Phi(t/4) - \pi/2 \sim -\pi \quad (15)$$

where  $\Phi(t)$  is the absolute phase of the elementary scattering amplitude

$$f(t) = |f(t)| e^{i\Phi(t)} \quad (16)$$

Since for high energy proton-proton elastic scattering  $\Phi(t) \sim \pi/2$  and it is varying slowly with the momentum transfer, the phase difference between the two phases is

This means that they interfere destructively. When the intensity of the two waves is of the same order, one should observe a complete cancellation between the two waves. This was predicted to occur for hadron deuteron elastic scattering for  $|t| \sim 0.3 \text{ GeV}^2$ , but it did not appear in the experimental data because of the presence of an incoherent contribution coming from the D wave of the deuteron<sup>17)</sup>. Nowadays, it is possible to use aligned deuteron beams and eliminate this incoherent contribution, recovering a high sensitivity to the absolute phase of the rescattered wave<sup>18)</sup>.

The application of hadron interferometry to the case of inelastic diffraction is not affected by the presence of the D wave of the deuteron as we shall see in the following. This application was done at ISR<sup>19)</sup>, where deuterons were stored and scattered with deuterons or protons. The measured reactions were

$$nd \rightarrow (\pi\pi^-) d \quad \sqrt{s} = 37 \text{ GeV} \quad (17)$$

$$pd \rightarrow (p\pi^+\pi^-) d \quad \sqrt{s} = 53 \text{ GeV} \quad (18)$$

and the method of analysis was based on Glauber theory<sup>19)</sup> taking into account one simple scattering amplitude and two double scattering amplitude, represented graphically in fig. 12. In the second double scattering diagram the intermediate state is the excited state of the nucleon and the second interaction is the elastic scattering of  $N^*$  on nucleon, which is taken in the analysis to be equal to the result of coherent production experiments on heavy nuclei.

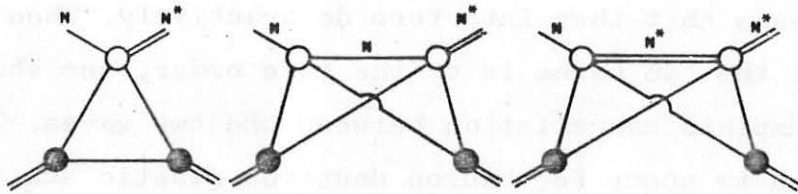


Fig. 12 Feynman graphs representing Glauber theory for coherent production.

The input amplitudes for inelastic diffractive are alternatively taken to be

- a) non-peripheral and purely helicity non-flip

$$f(t) = i(a_1 e^{b_1 t} + a_2 e^{b_2 t} e^{i\varphi_2}) \quad (19)$$

- b) peripheral and helicity flip dominated by the helicity non-flip part

$$f_\mu(t) = i c_\mu e^{at} J_\mu(R\sqrt{-t}) e^{i\mu\varphi} \quad (20)$$

For both amplitudes, the parameters are determined from a best fit of the proton-proton data for inelastic diffraction<sup>19)</sup>.

The corresponding contribution to the inelastic overlap function is given in fig. 13.

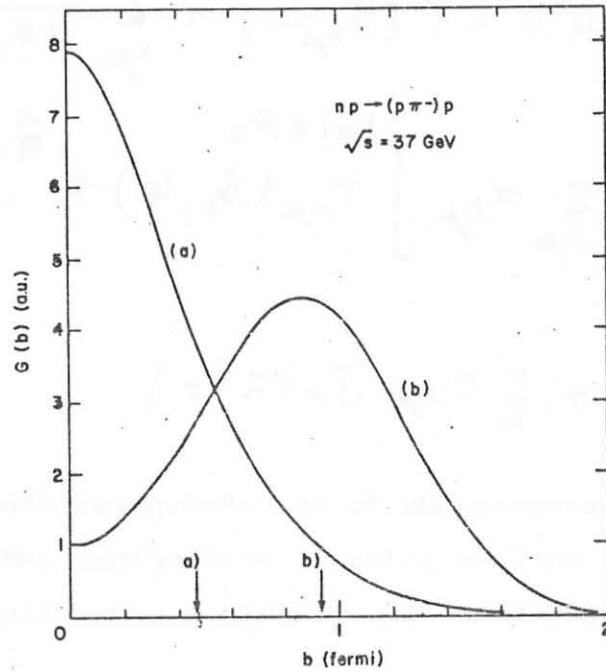


Fig. 13 Overlap function in impact parameter space of neutron single diffraction assuming central (a) and peripheral (b) amplitudes (see text). The arrows indicate the value of  $b_{rms}$  for both cases.

In the peripheral option (b), the form of the amplitude can be justified, using an absorption model from a deformed body, coming from nuclear physics<sup>3)</sup>. The surface of this body can be described by the following equation

$$R(\theta, \varphi) = R_0 \left( 1 + \sum_{\lambda \mu} \alpha_{\lambda \mu} Y_{\lambda \mu}(\theta, \varphi) + \dots \right) \quad (21)$$

as from the theory of the liquid drop with normal modes of excitation. The absorption amplitude is



$$\begin{aligned}
 F &= \int_{|b| \leq R(\pi_2, \theta)} e^{i\vec{q} \cdot \vec{b}} d^2b \cong F(\alpha_{\lambda\mu} = 0) + \sum_{\lambda\mu} \frac{\partial F}{\partial \alpha_{\lambda\mu}} \alpha_{\lambda\mu} \\
 &= R_0^2 \frac{J_1(qR_0)}{qR_0} + \sum_{\lambda\mu} \alpha_{\lambda\mu} \int_{|b| \leq R_0} Y_{\lambda\mu}(\pi_2, \varphi) e^{i\vec{q} \cdot \vec{b}} d^2b \\
 &= R_0^2 \frac{J_1(qR_0)}{qR_0} + \sum_{\lambda} c_{\lambda\mu} J_{\lambda}(qR_0)
 \end{aligned} \tag{22}$$

The first term corresponds to the absorption from the body with the equilibrium surface (elastic scattering) and the other terms to the absorption from the excitation modes (inelastic diffraction).

For this peripheral option (b) the Glauber theory for coherent production is

$$\begin{aligned}
 F_{\mu}(q) &= i c_{\mu}(M) \left[ 2 J_{\mu}(qR_0) e^{-2q^2} S'(q/2) \right. \\
 &+ \frac{i}{2P_{lab}} (f(b) + f^*(b)) \left. \right] \\
 &\times \sum A_i \frac{e^{-\frac{(\alpha_i + 4b)q^2}{4}}}{\alpha_i + b + a} \exp\left\{ \frac{(\alpha_i + 2b)q^2 - R_0^2}{4(\alpha_i + b + a)} \right\} J_{\mu} \left[ \frac{(\alpha_i + 2b)qR_0}{2(\alpha_i + b + a)} \right]
 \end{aligned} \tag{23}$$

In the double scattering term  $f(b)$  is the nucleon-nucleon elastic amplitude in the forward direction and  $f^*(b)$  the same for the  $N^*$ -nucleon case. The deuteron form factor is assumed to be a sum of gaussians

$$S'(q) = \sum_i A_i e^{-\alpha_i q^2} \tag{24}$$

From the above formula(23) it is clear that for the dominant  $\mu=0$  case the single scattering amplitude has a zero at small momentum transfers, but this zero is shifted to higher values of  $|t|$  in the double scattering term because the argument is

$$\frac{(d_1 + 2b) q R_0}{2(d_1 + b + a)} \sim \frac{q R_0}{2} \quad (25)$$

This situation produces a phenomenon of constructive interference in the differential cross section visible in fig. 15 for low values of the mass of the excited system. The non-peripheral option (a) for the input amplitude is not able to reproduce the features of the data, as shown by the dashed lines in fig. 14

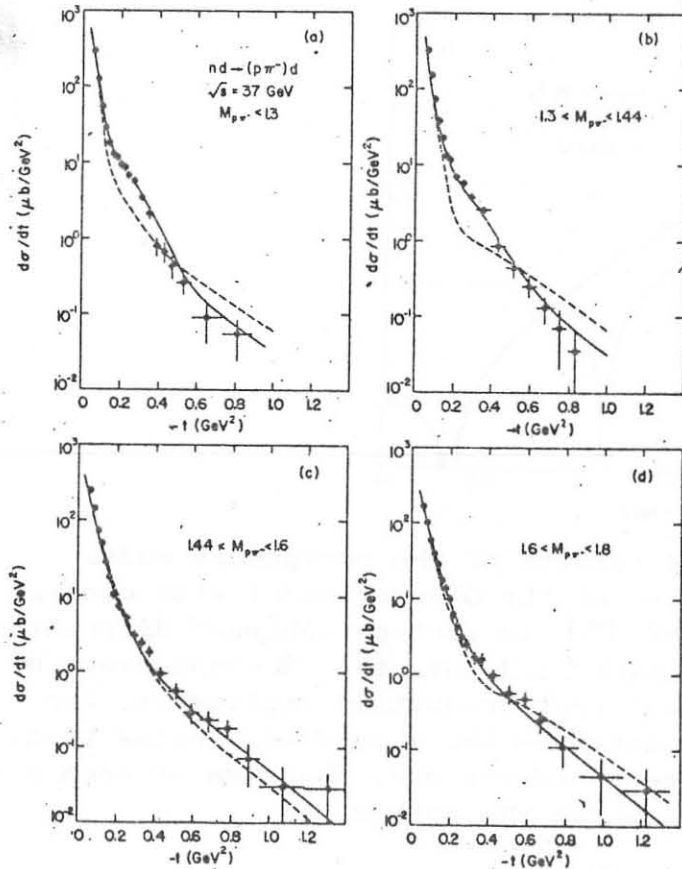


Fig. 14  
Differential cross sections for neutron coherent diffraction in four different mass bins. The continuous curves correspond to the peripheral model, the dashed curves to the central model.

Normalizing the cross section on the prediction of the non peripheral model, one obtains an impressive structure in correspondence to the region where the single and the double scattering amplitude have the same sign and are of the same order of magnitude. This is shown in fig. 15.

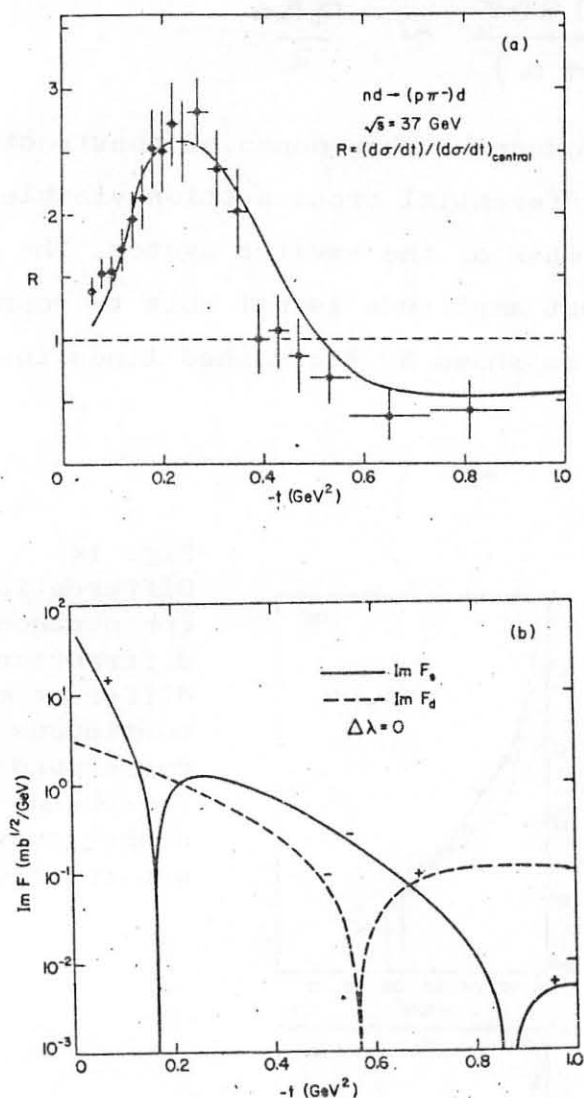


Fig. 15 (a) Data points and results of the peripheral model normalized to the predictions of the Glauber model with central amplitudes, as a function of  $|t|$  in neutron coherent diffraction for the mass interval  $M(p\pi^-) < 1.3$  GeV. (b)  $t$ -dependence of the imaginary part of the coherent production amplitudes, for  $\mu = 0$ . The continuous curve is the single-scattering term, the dashed curve the double-scattering one. The sign of each part of the amplitude is also shown on the curves.

The zeros of the scattering amplitude which should be visible for the dominant case  $\mu = 0$ , are actually hidden in the differential cross section by the incoherent contribution of the helicity flip ( $\mu \neq 0$ ) amplitudes. The dashed line of fig. 16 shows the zero of the  $\mu = 0$  contribution, and the continuous line the  $\mu \neq 0$  component; the helicity flip terms play a very important role in this game, at the zeros of the  $\mu = 0$  dominant amplitude

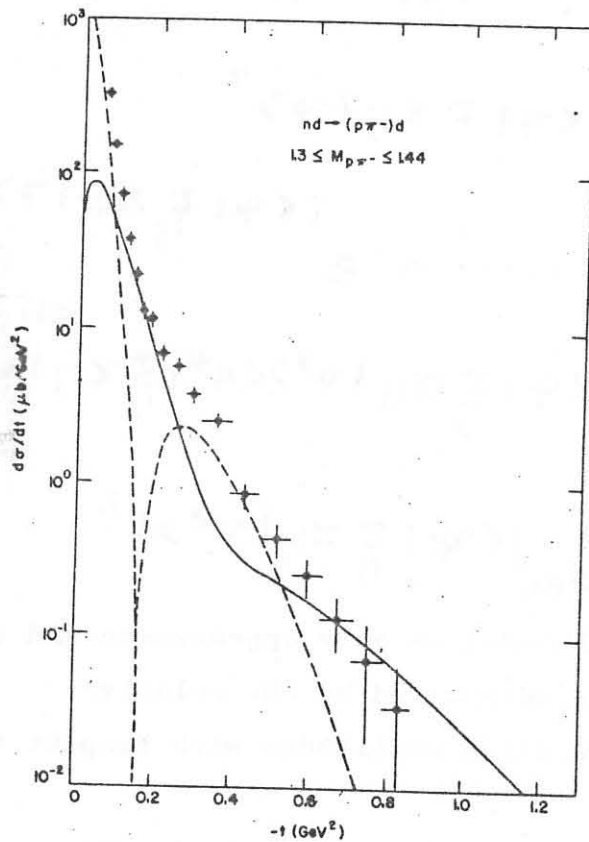


Fig. 16  
Differential cross section for coherent neutron diffraction in the second lowest mass bin. The curves represent two separate contribution to the peripheral-model calculation; the dashed line is the contribution of the  $\mu \neq 0$  amplitude, the continuous line the contribution of the helicity-flip terms.

This detailed analysis of the constructive interference phenomenon gives a clear cut proof that inelastic diffraction is peripheral. One can conclude therefore, that its large increase over the ISR energy range, explain most of the peripheral increase of the inelastic overlap function.

#### 4. INCLUDING INELASTIC DIFFRACTION IN THE EIKONAL MODEL

The eikonal model for elastic scattering, we have discussed above, may be substantially modified by the inclusion of inelastic states. This is known since a long time <sup>20)</sup> in the framework of Glauber theory. Indeed the average value of the eikonal function over the ground state of the nucleus is, expanding in power series

$$\begin{aligned}
 \langle \psi | e^{i \sum_{ij} \chi_{ij} (\vec{b}_i + \vec{b} - \vec{b}_j)} | \psi \rangle &= \\
 &= e^{i \langle \psi | \sum_{ij} \chi_{ij} | \psi \rangle} + \frac{1}{2} (\langle \psi | \sum_{ij} \chi_{ij} | \psi \rangle^2 \\
 &\quad - \langle \psi | (\sum_{ij} \chi_{ij})^2 | \psi \rangle) + \dots \sim e^{i \langle \psi | \sum_{ij} \chi_{ij} | \psi \rangle} \\
 &\quad + \frac{1}{2} (\langle \psi | \sum_{ij} \chi_{ij} | \psi \rangle^2 - \sum_{\psi^*} \langle \psi | \sum_{ij} \chi_{ij} | \psi^* \rangle \langle \psi^* | \sum_{ij} \chi_{ij} | \psi \rangle) \\
 &= e^{i \langle \psi | \sum_{ij} \chi_{ij} | \psi \rangle} - \frac{1}{2} \sum_{\psi^* \neq \psi} |\langle \psi | \sum_{ij} \chi_{ij} | \psi^* \rangle|^2
 \end{aligned} \tag{26}$$

This means that the eikonal model is only approximate and the goodness of the approximation is determined by the relative importance of the inelastic transition amplitudes with respect to the elastic one.

This result is however not useful for proton inelastic diffraction, because of the difficulty of Glauber theory in reproducing the diffractive peak of fig. 3. The reason is that in the impulse approximation the transition amplitude is <sup>7)</sup>

$$\langle \psi^* | e^{i \sum_i \vec{q}_i \cdot \vec{b}_i} | \psi \rangle = 0 \quad \text{for } \vec{q} = 0 \tag{27}$$

and multiple scattering corrections partially fill the zero but

leave a dip in the forward direction.

In order to include, at least implicitly, in the eikonal model inelastic diffraction one may represent the proton as a superposition of states with different numbers of partons<sup>21)</sup>

$$\begin{aligned}
 |\psi\rangle = & c_0 |0\rangle + \sum_i \int d^3p c_{\tau i}(p) a_i^*(p) |0\rangle \\
 & + \sum_{i,j} \int d^3p_1 d^3p_2 c_{2ij}(\vec{p}_1, \vec{p}_2) a_i^*(p_1) a_j^*(p_2) |0\rangle + \dots
 \end{aligned}
 \tag{28}$$

and one may assume that dressed states interact more strongly than bare states; in this way the picture of Good and Walker<sup>4)</sup> acquires a precise physical meaning. It is clear that the eikonal model becomes inconsistent with this scheme, if we insist on assuming that the eikonal function is the overlap between the matter distributions and these matter distributions refer now to the particular component states of the proton<sup>22)</sup>. This is the obvious generalization of the hypothesis of Chou-Yang<sup>8)</sup> to the fluctuating picture of the nucleon.

In this scheme the profile function becomes<sup>22)</sup>

$$\begin{aligned}
 \sum_{ij} \{1 - \exp(-\Omega_{ij}(b))\} c_{ij} &= \\
 = 1 - e^{-\langle \Omega \rangle} \sum_{\alpha=0}^{\infty} \frac{(-)^{\alpha}}{\alpha!} \mu_{\alpha}(b)
 \end{aligned}
 \tag{29}$$

where

$$\mu_{\alpha}(b) = \langle \Omega(b) - \langle \Omega(b) \rangle^{\alpha} \rangle
 \tag{30}$$

The eikonal function  $\langle \Omega \rangle$  would now correspond to the Chou-Yang overlap function between the matter distributions, because

it is averaged on all the components of the nucleon state. It is clear however that the eikonal form is not consistent with the hypothesis (28), because of the non zero value for the forms  $\mu_{\alpha}(b)$ . These terms are clearly non zero for , because of the fluctuations of the nucleon field. Actually for

$$\mu_2(b) = \langle \Omega^2(b) \rangle - \langle \Omega(b) \rangle^2 \quad (31)$$

which can be interpreted as impact parameter distribution of inelastic diffraction cross section. Indeed, expanding the exponential in the first line of (29), the eigenvalue  $t_i$  for the state  $i$  is

$$T_{ii}(b) = 1 - e^{-\Omega_{ii}(b)} \sim \Omega_{ii}(b) \quad (32)$$

since the total inelastic diffraction is given by

$$\begin{aligned} \sigma_{diff} &= \sum_{\psi_d^* \neq \psi} |\langle \psi_d^* | T | \psi \rangle|^2 = \\ &= \sum_{\psi_d^*} |\langle \psi_d^* | T | \psi \rangle|^2 - |\langle \psi | T | \psi \rangle|^2 \\ &= \sum_i \langle i | T^2 | i \rangle - \left| \sum_i \langle i | T | i \rangle \right|^2 \end{aligned} \quad (33)$$

The above expression (31) is then the impact parameter distribution of inelastic diffraction and the eikonal picture of Chou and Yang is consistent with zero value for inelastic diffraction, in this particular scheme. On the other side this scheme, seems to be the only one, capable to reproduce easily the diffractive peak of inelastic diffraction<sup>7)</sup>. Expression (29) seems

now the most suitable generalization of the eikonal model, which includes explicitly inelastic diffraction. This is however not the solution of the problem, because we are not able to determine the coefficients  $C_{ij}$  and the eikonal function  $\Omega_{ij}(b)$ , unless we solve the confinement problem for hadrons and we understand strong interactions at large distances.

In the arbitrary scheme of ref. 22, one uses the following ansatz

$$\sum_{ij} C_{ij} \Omega_{ij}(b) = P(b) \Omega(b) \quad (34)$$

where

$$P(b) = K \frac{\Omega^\alpha(b)}{\langle \Omega(b) \rangle^\alpha} e^{-\frac{\lambda \Omega(b)}{\langle \Omega(b) \rangle}} \quad (35)$$

In order to obtain the right value of inelastic diffraction one has to assume that the matter density in the proton is completely different than the charge density, that is the matter is more dense than charge at small distances. The result of ref. 22 is reported in fig. 17, where the matter distribution for two different values of  $\sigma_{diff}$  is compared with the distribution, as obtained from electron proton scattering.

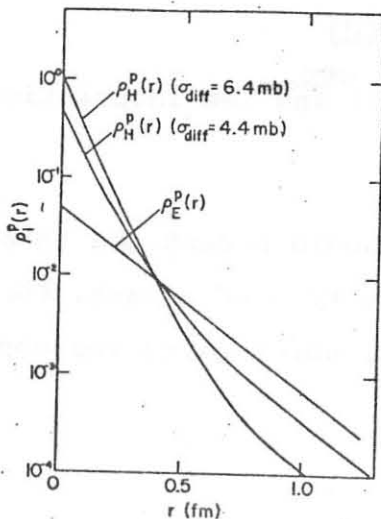


Fig. 17  
Matter distribution for the proton compared with charge distribution<sup>22</sup>).



The figure shows that the hadronic matter is more dense at small values of  $b$  than the charge, which could be considered as a proof for the MIT bag model or for the string model, where two external quarks emit a gluon flux, which connect their positions (fig. 18)

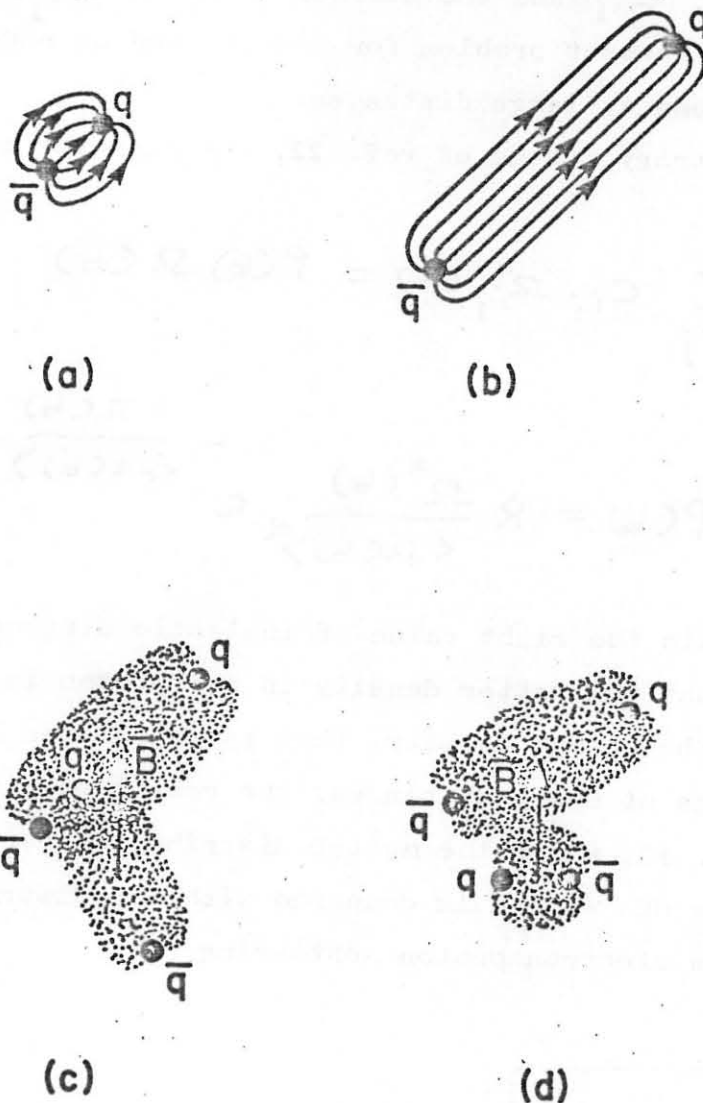


Fig. 18 String picture of the pion (a,b) and the interaction mechanism (c,d)

It is not clear however, why we should accept the ansatz (34) and how sensitive is this result to the type of ansatz. For instance, can we think about an ansatz, which gives the opposite result for the matter distribution?

This is still an unanswered question and worth investigating, but the result of ref. 22 seems very encouraging and indicates in the study of diffraction a useful tool for investigating the proton structure in terms of quarks and gluons.

## 5. SUMMARY

We have collected in this review a number of experimental facts and theoretical ideas, in the hope of drawing a definite conclusion from the activity on proton-proton diffraction in the last decade.

This conclusion is not easy to be drawn, because, while much is known about the empirical features of proton-proton diffraction, a satisfactory theoretical picture is still missing.

Some qualitative aspects of this picture, however, emerge clearly from our discussion; they refer to the fluctuating structure of hadrons, as confined quark bound states continuously emitting gluons.

This structure is related to the difficulty of Glauber theory in reproducing the diffractive peak in inelastic diffraction. Also the inability of eikonal models in reproducing the highly non uniform increase with  $S$  of the inelastic overlap function, is related to inelastic diffraction, because this seem to be the most important cause of this effect. Indeed the peripheral increase of  $G_{\mu}(b)$ , could be explained by a corresponding increase in inelastic diffraction, which is shown to be peripheral in an independent way.

It becomes then important to generalize eikonal models in order to include implicitly inelastic diffraction. The first trial in this direction gives as natural consequence a large difference between charge and matter distribution in the proton.

It is clear that much remain to be done in this direction and for this purpose the full potential of gauge theories and confining models for hadrons should be exploited.

## AKNOWLEDGEMENTS

I'm grateful to CNPq and COPPE-UFRJ for making possible my visit at Instituto de Física, UFRJ, Rio de Janeiro, where this work found its final form.

References

1. H.D.I. Abarbanel, Review of Mod. Phys. 48 (1976) 435.
2. F. Low, Phys. Rev. D 12 (1975) 163.
3. G. Alberi and G. Goggi, "Diffraction of subnuclear waves", to appear in Phys. Reports.
4. M.L. Good and W.D. Walker, Phys. Rev. 120 (1960) 1857.
5. U. Amaldi, M. Jacob and G. Matthiae Ann. Rev. of Nucl. Science 26 (1976) 385.
6. R.P. Feynman, "Photon Hadron Interactions", Benjamin Inc. Reading, 1973.
7. H. Miettinen and J. Pumplin, Phys. Rev. D18 (1978), 1696.
8. T.T. Chou and C.N. Yang, Phys. Rev. 170 (1968) 1591.
9. J. Saudinos and C. Wilkin Ann. Rev. of Nucl. Science 24 (1974) 341.
10. D.J. Clarke and S.Y. Lo, Phys. Rev. D10 (1974) 1519.
11. H.M. França et al., University of Sao Paulo Preprint, January 1980.
12. R.J. Clarke and S.Y. Lo, Phys. Lett. 87B (1979) 379
13. C. Bourelly et al. Physics Reports C59 (1980)95
14. U. Amaldi in Proc. of Int. conf. on High Energy Physics, Aix en Provence, 1973.
15. H.M. França and Y. Hama Phys. Rev. D19(1979) 3261.
16. U. Amaldi and K. Schubert CERN preprint 1979.
17. L. Bertocchi in Proc. of the Summer School on High Energy Physics, Hercegnovi, 1969.
18. G. Alberi et al. Phys. Lett. 92B(1980) 41  
S. Santos, communication to this meeting
19. G. Goggi et al. Nucl. Phys. B161 (1979) 14.
20. N. Byers and S. Frautschi in "Quanta, ed. Chicago Univ. Press
21. R.P. Feynman Proc. of the Haway Topical Conference in High Energy Physics, Honolulu, 1977.
22. H. Miettinen and G. Thomas Nucl. Phys. B166 (1980)365